JOURNAL OF MATERIALS SCIENCE 35 (2000) 3711–3717

The effect of heat-treatment on the grain-size of nanodisperse plasmathermal silicon nitride powder

J. GUBICZA
Department of General Physics, Eötvös University, Budapest, P.O. Box 32, H-1518, Hungary

J. SZÉPVÖLGYI, I. MOHAI
Research Laboratory of Materials and Environmental Chemistry, Chemical Research Center, Hungarian Academy of Sciences, Pusztaszeri út 59-67, Budapest, H-1025, Hungary

G. RIBÁRIK, T. UNGÁR*
Department of General Physics, Eötvös University, Budapest, P.O. Box 32, H-1518, Hungary
E-mail: ungar@ludens.elte.hu

Nanodisperse silicon nitride has been synthesized by vapor phase reaction of silicon tetrachloride and ammonia in a thermal plasma reactor and crystallized at temperatures 1250, 1350, 1450 and 1500°C. The average grain-size and the dislocation density of the samples were determined by the recently developed *modified* Williamson-Hall and Warren-Averbach procedures from X-ray diffraction profiles. A new numerical method provided log-normal grain-size distributions from the size parameters derived from X-ray diffraction profiles. It has been shown that the average grain-size in the amorphous phase is lower than that observed in the crystalline fraction. On the other hand, the average grain-size in the crystalline fraction decreases up to 1450°C while it increases during heat-treatment at 1500°C. The size distribution and the area-weighted average grain-size obtained by X-rays were in good agreement with those determined by TEM and from the specific surface area, respectively. The dislocation density was found to be of the order of 10^{14} and 10^{15} m^{-2}.

1. Introduction

Dense silicon nitride ceramics are important structural materials because of their good room and high temperature mechanical properties. Silicon nitride powders produced in thermal plasmas are predominantly amorphous with a minor crystalline phase content due to the very rapid cooling downwards the plasma flame region [1]. The amorphous silicon nitride powders can be processed in different ways to produce dense ceramics. The traditional way involves annealing of powders to produce crystalline material having high α-Si_3N_4 content that can be doped, compacted and sintered at high temperatures [2]. Consequently, studying the crystallization of amorphous thermal plasma powders is very important from both the theoretical and practical point of view. The average grain-size and the grain-size distribution of the crystallized powders have a great influence on the density, the phase composition and the microstructure, and therefore on the mechanical properties of the resulting ceramics [3–5]. Cambier *et al.* have found that the density of the specimen at the beginning of sintering is larger if the grain-size distribution of the starting powder is wider [5]. It has been also established that during sintering the densification depends mainly on the inverse of the average grain-size. On the other hand, if the grain-size distribution at the beginning is wide then coarsening of the grains can occur leading to lower sinterability as densification proceeds [5]. Consequently, the investigation of the changes of the average grain-size and the grain-size distribution of the thermal plasma powders during crystallization has particular relevance.

The grain-size of silicon nitride powder can be measured by transmission electron microscopy (TEM), however this is a laborious and time consuming procedure. Furthermore, the volume that one can examine in a microscope is always very small in comparison with the entire sample leading to uncertainty as to whether a truly characteristic region of the sample was investigated. On the other hand, X-ray diffraction examines a much larger fraction of the specimen, and the preparation of the sample and the evaluation of the measurements are not so laborious. Krill and Birringer have recently developed a procedure to determine size distribution from the Fourier transform of X-ray diffraction profiles [6]. In this procedure, however, the anisotropic

* Author to whom all correspondence should be addressed.

strain broadening has not been accounted for and only the Fourier coefficients of the diffraction profiles were used. It has been shown recently that strain anisotropy can be well accounted for by the dislocation model of the mean square strain [7–13]. The model described in these papers takes into account that the contrast caused by dislocations depends on the relative directions of the line and Burgers vectors of the dislocations and the diffraction vector, respectively. Anisotropic contrast can thus be summarised in contrast factors, C, which can be calculated numerically on the basis of the crystallography of dislocations and the elastic constants of the crystal [9–13]. By appropriate determination of the type of dislocations and Burgers vectors present in the crystal, the average contrast factors, $\bar{C}$, for the different Bragg reflections can be determined. Using the average contrast factors in the *modified* Williamson-Hall plot and in the *modified* Warren-Averbach procedure, the different averages of grain-sizes and the dislocation density can be obtained [7, 8]. In a recently published paper a new pragmatical and self-consistent procedure has been proposed for the stable determination of grain-size distribution using the three size parameters obtained from the full widths at half maximum (FWHM), the integral breadths and the Fourier coefficients of the diffraction profiles [14].

The aim of the present paper is i) to investigate the correlation between the grain-size distribution determined by TEM measurements, the average grain-size calculated from the specific surface area and those obtained by the recently developed X-ray diffraction procedure and ii) to study the influence of the crystallization temperature on the average grain-size and the grain-size distribution of the silicon nitride powders produced in a thermal plasma reactor.

2. Experimental details

2.1. Powder preparation

Silicon nitride powder was synthesized by the vapor-phase reaction of silicon tetrachloride and ammonia in a radiofrequency thermal plasma reactor under conditions given previously [15, 16]. The as-synthesized powder was subjected to a two-step thermal processing to remove NH_4Cl and $Si(NH)_2$ by-products formed due to the NH_3 excess in the plasma synthesis. The powder was treated in nitrogen at 400°C for 1 h and subsequently at 1100°C for 1 h to achieve the complete decomposition of by-products. This resulting powder was predominantly amorphous with a crystalline content of about 20 vol%. The crystallization was performed in a horizontal laboratory furnace in flowing nitrogen at 0.1 MPa, at annealing temperatures of 1250, 1350, 1450 and 1500°C for 2 h.

2.2. X-ray diffraction technique

The crystalline phases were identified by X-ray diffraction (XRD) using a Guinier-Hagg focusing camera and Cu $K_{\alpha 1}$ radiation. The relative amounts of α- and β-Si_3N_4 phases were determined from the XRD pattern using the Gazzara and Messier method [17]. In this procedure the intensities of the 201, 102 and 210 reflections of α-Si_3N_4 and the 200, 101 and 210 reflections of β-Si_3N_4 were averaged to minimize preferred orientation effects and statistical errors. The ratio of the amounts of α- and β-Si_3N_4 phases was calculated from these averaged intensities using the formula proposed by Camuscu *et al.* [18].

The diffraction profiles were measured by a special double crystal diffractometer with negligible instrumental broadening [7, 19]. A fine focus rotating cobalt anode (Nonius FR 591) was operated as a line focus at 36 kV and 50 mA ($\lambda = 0.1789$ nm). The symmetrical 220 reflection of a Ge monochromator was used in order to have wavelength compensation at the position of the detector. The $K_{\alpha 2}$ component of the Co radiation was eliminated by an 0.16 mm slit between the source and the Ge crystal. By curving the Ge crystal sagittally in the plane perpendicular to the plane-of-incidence the brilliance of the diffractometer was increased by a factor of 3. The profiles were registered by a linear position sensitive gas flow detector, OED 50 Braun, Munich. In order to avoid air scattering and absorption the distance between the specimen and the detector was overbridged by an evacuated tube closed by mylar windows.

Transmission electron microscopy (TEM, JEOL JEM200CX) has been used for direct measurement of the grain-size and size distribution. Bright field images of the grains were used to measure the grain-size in powder samples.

The specific surface areas of the powders were determined from the nitrogen adsorption isotherms by the BET (Brunauer-Emmett-Teller) method [20]. Assuming that the grains have spherical shape, the area-weighted average grain-size (t) in nanometers was calculated as $t = 6000/qS$ where q is the density in g/cm^3 and S is the specific surface area in m^2/g.

3. Evaluation of the X-ray diffraction profiles

3.1. The modified Williamson-Hall and Warren-Averbach methods

Assuming that strain broadening is caused by dislocations the full widths at half maximum (FWHM) of diffraction profiles can be given by the *modified* Williamson-Hall plot as [7, 8]:

$$\Delta K = \frac{\gamma}{D} + \alpha(K\bar{C}^{1/2}) + O(K^2\bar{C}), \qquad (1)$$

where D is a size parameter characterising the column lengths in the specimen, γ equals to 0.9, α is a constant depending on the effective outer cut-off radius, the Burgers vector and the density of dislocations, $\bar{C}$ is the contrast factor of dislocations depending on the relative positions of the diffraction vector and the Burgers and line vectors of the dislocations and on the character of dislocations [7, 9–13] and O stands for higher order terms in $K\bar{C}^{1/2}$. K is the length of the diffraction vector: $K = 2\sin\theta/\lambda$, where θ is the diffraction angle and λ is the wavelength of X-rays. $\Delta K = \cos\theta[\Delta(2\theta)]/\lambda$, where $\Delta(2\theta)$ is the FWHM of the diffraction peak. The size parameter corresponding to the FWHM, D, is obtained from the intercept at

$K = 0$ of a smooth curve according Equation 1 [7]. The modified Williamson-Hall procedure was also applied for the integral breadths of the profiles. In this case γ was taken as 1 and the obtained size parameter denoted by d gives the volume-weighted average column length in the sample [21]. We note that in the present case shape isotropy is assumed which holds to a great extent as supported by TEM observations.

$\bar{C}$ is the weighted average of the individual C factors over the dislocation population in the crystal. In the present case the C factors could not be calculated directly since, to the knowledge of the authors, the anisotropic elastic constants of Si_3N_4 are not available. Therefore the average $\bar{C}$ factors were determined by the following indirect method. Based on the theory of line broadening caused by dislocations it has been shown that the average dislocation contrast factor in an untextured hexagonal polycrystalline specimen is the following function of the invariants of the fourth order polynomials of Miller indices hkl [22]:

$$\bar{C} = \bar{C}_{hk0}\left[1 + \frac{[A(h^2+k^2+(h+k)^2) + Bl^2]l^2}{[h^2+k^2+(h+k)^2+\frac{3}{2}\left(\frac{a}{c}\right)^2 l^2]^2}\right], \tag{2}$$

where $\bar{C}_{hk0}$ is the average dislocation contrast factor for the $hk0$ reflections, A and B are parameters depending on the elastic constants and on the character of dislocations in the crystal and c/a is the ratio of the two lattice constants of the hexagonal crystal ($c/a = 0.7150$ and 0.3826 for α- and β-Si_3N_4, respectively [23]). Inserting Equation 2 into Equation 1 the latter one was solved for D, α, A and B by the method of least squares. As $\bar{C}_{hk0}^{1/2}$ is a multiplier of K in Equation 1, its value can not be determined by this method. The value of $\bar{C}_{hk0}$ was calculated numerically assuming elastic isotropy because of the lack of the knowledge of anisotropic elastic constants. The isotropic $\bar{C}_{hk0}$ factor was evaluated for the most commonly observed dislocation slip system in silicon nitride [23]: $\langle 0001\rangle\ \{10\bar{1}0\}$. Taking 0.24 as the value of the Poisson's ratio [24] $\bar{C}_{hk0} = 0.0279$ was obtained for both α- and β-Si_3N_4.

The *modified* Warren-Averbach equation is [7]:

$$\ln A(L) \cong \ln A^S(L) - \rho B L^2 \ln(R_e/L)(K^2\bar{C}) + O(K^4\bar{C}^2), \tag{3}$$

where $A(L)$ is the real part of the Fourier coefficients of the diffraction profiles, A^S is the size Fourier coefficient as defined by Warren [25], ρ is the dislocation density, $B = \pi b^2/2$ (b is the length of the Burgers vector), R_e is the effective outer cut-off radius of dislocations and O stands for higher order terms in $K^2\bar{C}$. L is the Fourier length defined as [25]:

$$L = na_3, \tag{4}$$

where $a_3 = \lambda/2(\sin\theta_2 - \sin\theta_1)$, n are integers starting from zero, λ is the wavelength of X-rays and $(\theta_2 - \theta_1)$ is the angular range of the measured diffraction profile. The average dislocation contrast factors $\bar{C}$ determined from the *modified* Williamson-Hall plot of FWHM were also used in Equation 3. The size parameter corresponding to the Fourier coefficients is denoted by L_0. It is obtained from the size Fourier coefficients, A^S, by taking the intercept of the initial slope at $A^S = 0$ [25] and it gives the area-weighted average column length [21]. Assuming that the grains are spherical, the area-weighted average grain-size of the crystalline phases ($\langle x\rangle^c_{area}$) was calculated from the area-weighted average column length as follows: $\langle x\rangle^c_{area} = 3L_0/2$ [6, 26, 27].

The area-weighted average grain-size of the amorphous phase was calculated from those of the entire powder (t) and the crystalline fraction ($\langle x\rangle^c_{area}$) as follows. For spherical grains the area-weighted average grain size of a powder sample can be obtained as the ratio of the third and the second moments of the grain-size distribution $f(x)$ [6]:

$$\langle x\rangle_{area} = \frac{\int_0^\infty x^3 f(x)\,dx}{\int_0^\infty x^2 f(x)\,dx} = \frac{6V}{A}, \tag{5}$$

where V is the volume and A is the surface area of the sample. Assuming for our specimens that the surface area of the entire powder (A_e) equals to the sum of the surface areas of the crystalline (A_c) and the amorphous (A_a) fractions and using Equation 5 one can get

$$\frac{(V_c + V_a)}{t} = V_c/\langle x\rangle^c_{area} + \frac{V_a}{\langle x\rangle^a_{area}}, \tag{6}$$

where V_c and V_a are the volumes, $\langle x\rangle^c_{area}$ and $\langle x\rangle^a_{area}$ are the area-weighted average grain-sizes of the crystalline and the amorphous fractions of the powder, respectively, and t is the area-weighted average grain-size of the entire powder. Rearranging Equation 6 the following equation can be obtained for the average grain-size of the amorphous fraction

$$\langle x\rangle^a_{area} = \frac{V_a}{V_c}\frac{1}{\left[\frac{1}{t}\left(1+\frac{V_a}{V_c}\right) - \frac{1}{\langle x\rangle^c_{area}}\right]}. \tag{7}$$

Using Equation 7 the determination of the area-weighted average grain-size of the amorphous fraction for the samples having small amount of amorphous phase is uncertain. Therefore the area-weighted average grain-size of the amorphous fraction was determined only for the powders having high amorphous phase content.

3.2. Determination of grain-size distribution from X-ray diffraction

Three size parameters were determined by the *modified* Williamson-Hall and Warren-Averbach procedures: D from the FWHM, d from the integral breadths and L_0 from the Fourier coefficients. These three gauges are stable and only restrictedly sensitive to experimental errors or fluctuations [13]. In a recent work a pragmatical and self-consistent numerical procedure has been worked out to relate the experimentally determined D,

d and L_0 values to the parameters of a grain-size distribution function, $f(x)$ [14]. A brief description of this procedure is given below. It was observed by many authors that the grain-size distribution of nanocrystalline materials is log-normal [6, 14, 28]:

$$f(x) = \frac{1}{\sqrt{2\pi}\ln\sigma}\frac{1}{x}\exp\left\{-\frac{[\ln(x/m)]^2}{2\ln^2\sigma}\right\}, \quad (8)$$

where x is the grain-size, σ is the variance and m is the median of the size distribution function $f(x)$. Guinier has shown that if the crystallites are distortion free the Bragg peak profile can be described as [21]:

$$I(s) = \int_0^\infty \frac{\sin^2(\pi Ms)}{M(\pi s)^2} g(M)\,\mathrm{d}M, \quad (9)$$

where $s = \Delta(2\theta)/\lambda$, M is the column length and $g(M)$ is the volume fraction distribution function of the columns in the sample. The $g(M)\mathrm{d}M$ represents the volume fraction of the columns for which the length parallel to the diffraction vector lies between M and $M + \mathrm{d}M$. As can be seen from Equation 9, X-ray diffraction directly measures the volume fraction distribution of the column lengths. The relationship between $g(M)$ and $f(x)$ depends on the shape of the crystallites since the volume fraction of the column lengths in a given grain is related to the geometric boundaries of the grain. The shape of the grains was approximated by spheres supported by TEM observations. For spherical grains the relationship between $g(M)$ and $f(x)$ can be given in the following form:

$$g(M) = NM^2\int_M^\infty f(x)\,\mathrm{d}x, \quad (10)$$

where N is a normalization factor. Substituting Equation 8 into Equation 10, calculating the integral in Equation 10 and substituting Equation 10 into Equation 9, for the intensity distribution one obtaines:

$$I(s) = \int_0^\infty M\frac{\sin^2(\pi Ms)}{2(\pi s)^2}\mathrm{erfc}\left[\frac{\ln(M/m)}{\sqrt{2}\ln\sigma}\right]\mathrm{d}M, \quad (11)$$

where erfc is the complementary error function. It can be seen from Equation 11 that the shape of the peak profile depends on σ and m. The parameters σ and m corresponding to our samples were determined from Equation 11 by a computer program satisfying the condition that the sum of the squares of the difference between the D, d and L_0 of the numerically calculated $I(s)$ function and the experimental values of these parameters is minimum.

4. Results and discussion

The phase composition of the powders can be seen in Table I. The X-ray phase analysis shows that the major phase is α-Si_3N_4. Beside this phase β-Si_3N_4 was also identified in the powders. It can be established that

TABLE I The phase composition of the as-synthesized and the heat-treated powders

Temperature of heat-treatment	amorphous (vol%)	α-Si_3N_4 (vol%)	β-Si_3N_4 (vol%)
as-synthesized	80	17	3
1250°C	70	27	3
1350°C	65	32	3
1450°C	25	67	8
1500°C	20	67	13

at crystallization temperatures up to 1350°C α-Si_3N_4 crystallized from the predominantly amorphous silicon nitride powder while the amount of β-Si_3N_4 did not change. At temperatures above 1350°C the crystalline content of the samples became very high ($\geq$75 vol%) and both α- and β-Si_3N_4 crystallized from the amorphous phase. In samples heat-treated up to 1350°C the β-Si_3N_4 phase will be neglected in the calculation of average grain-size and grain-size distribution because of its small amount compared with α-Si_3N_4.

The *modified* Williamson-Hall plots of the FWHM and the integral breadth for α-Si_3N_4 phase in powder crystallized at 1500°C are shown in Figs 1 and 2,

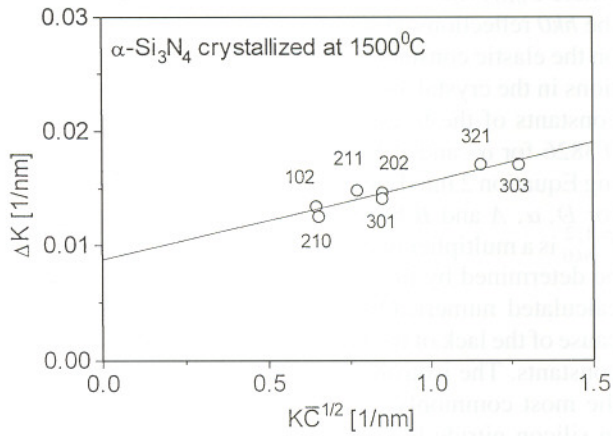

Figure 1 The FWHM as a function of $K\bar{C}^{1/2}$ for α-Si_3N_4 in powder crystallized at 1500°C according to the modified Williamson-Hall plot in Equation 1. The Miller indices of the reflections are also indicated.

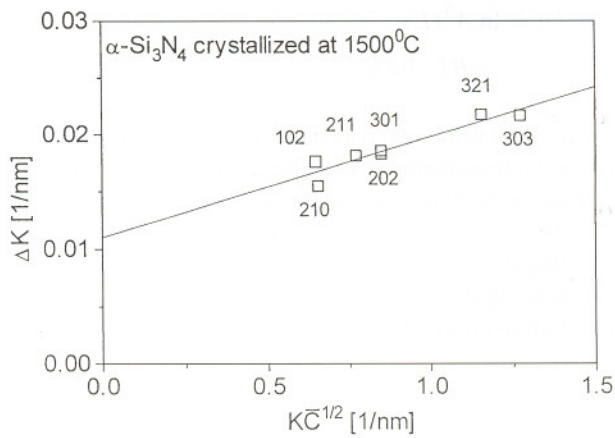

Figure 2 The integral breadth as a function of $K\bar{C}^{1/2}$ for α-Si_3N_4 in powder heat-treated at 1500°C according to the modified Williamson-Hall plot in Equation 1. The Miller indices of the reflections are also indicated.

TABLE II The values of the three size parameters D, d, L_0 determined from the FWHM, the integral breadth and the Fourier coefficients of the X-ray diffraction profiles, respectively; the area-weighted average grain-size obtained from X-rays ($\langle x\rangle^{c}_{area}$) and calculated from the specific surface area (t); the two parameters characterizing the log-normal size distribution functions, σ and m; and the dislocation density (ρ) in powders heat-treated at different temperatures

temperature of heat-treatment		D [nm]	d [nm]	L_0 [nm]	$\langle x\rangle^{c}_{area}$ [nm]	t [nm]	m [nm]	σ	ρ [m^{-2}]
as-synthesized	α-Si_3N_4	108 ± 5	88 ± 5	49 ± 3	74 ± 5	35 ± 2	26 ± 3	1.88 ± 0.07	4.9×10^{14}
1250°C	α-Si_3N_4	113 ± 4	89 ± 5	48 ± 4	72 ± 6	51 ± 3	23 ± 3	1.95 ± 0.08	1.2×10^{15}
1350°C	α-Si_3N_4	102 ± 5	72 ± 3	40 ± 3	60 ± 5	52 ± 3	16 ± 2	2.03 ± 0.08	1.8×10^{14}
	α-Si_3N_4	96 ± 4	70 ± 4	42 ± 4					7.7×10^{14}
1450°C					63 ± 6	75 ± 3	18 ± 2	1.95 ± 0.07	
	β-Si_3N_4	82 ± 5	67 ± 3	40 ± 4					3.6×10^{15}
	α-Si_3N_4	103 ± 4	91 ± 4	62 ± 4					5.7×10^{14}
1500°C					93 ± 6	94 ± 3	53 ± 7	1.60 ± 0.07	
	β-Si_3N_4	99 ± 5	94 ± 4	57 ± 3					7.1×10^{15}

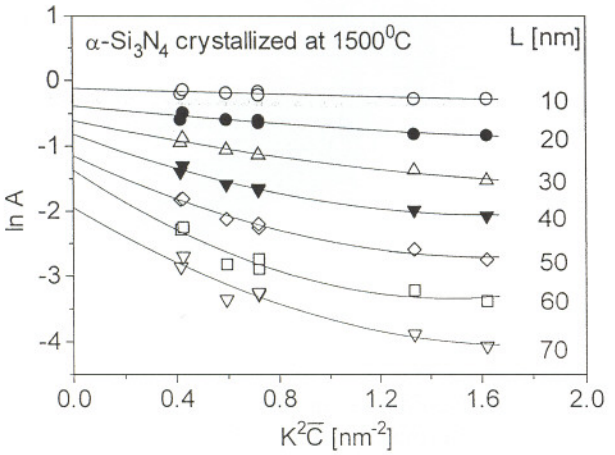

Figure 3 The logarithm of the real part of the Fourier coefficients versus $K^2\bar{C}$, for α-Si_3N_4 in powder crystallized at 1500°C according to the modified Warren-Averbach plot in Equation 3.

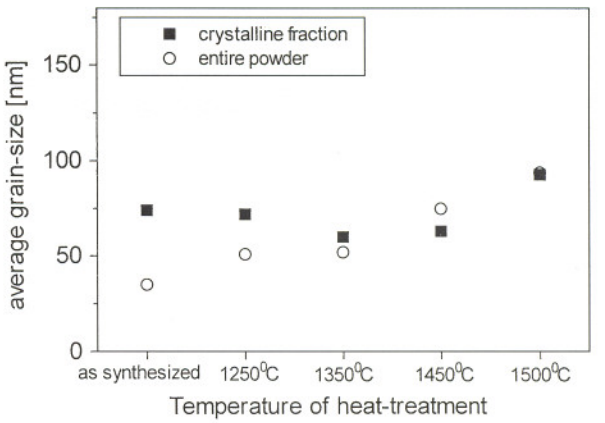

Figure 4 The area-weighted average grain-size of the crystalline fraction and that of the entire powder heat-treated at different temperatures.

respectively. The linear regressions to the FWHM and the integral breadth give $D = 103$ nm and $d = 91$ nm, respectively. The results obtained from similar procedures for α-Si_3N_4 and β-Si_3N_4 in the as-synthesized and the crystallized powders are listed in Table II.

A typical plot according to the *modified* Warren-Averbach procedure given in Equation 3 is shown in Fig. 3 for α-Si_3N_4 in sample crystallized at 1500°C. From the quadratic regressions the particle size coefficients, A^S were determined. The intersections of the initial slopes at $A^S(L) = 0$ yield the area-weighted average column length: $L_0 = 62$ and 57 nm for α-Si_3N_4 and β-Si_3N_4. The values of L_0 for the powders can be seen in Table II. It can be established that in samples heat-treated at 1450 and 1500°C the size parameters of α-Si_3N_4 are very close to those of β-Si_3N_4, therefore the average grain-size and the grain-size distribution calculated for the major α-Si_3N_4 phase were taken as characteristic parameters for the entire crystalline fraction of these samples. The area-weighted average grain-size calculated from L_0 for the crystalline fraction ($\langle x\rangle^{c}_{area}$) is shown in Table II. The area-weighted average grain-size of the entire powder (t) can be also seen in Table II. The area-weighted average grain-size of the amorphous phase ($\langle x\rangle^{a}_{area}$) was calculated from Equation 7 for the powders having high amorphous fraction. The values of the amorphous average grain-size are 31, 45 and 49 nm for the as-synthesized sample, the powders heat-treated at 1250 and 1350°C, respectively. It can be established that in these samples the average particle size of the amorphous phase is lower than that of the crystalline fraction and it increased during heat-treatments. The average size of the crystalline grains decreased slightly at temperatures up to 1450°C probably because of the crystallization of the smaller amorphous grains, while it significantly increased during heat-treatment at 1500°C (see Fig. 4). The average grain-size of the entire powder (t) increased with increasing temperature that is caused by the grain-coarsening in the amorphous phase and the increase of the amount of the crystalline phase having large grains. For the powder having high amount of crystalline phases (crystallized at 1500°C) the average grain-size of the crystalline fraction obtained by X-rays agrees well with that of the entire powder calculated from the specific surface area.

Log-normal particle size distribution functions were determined for the crystalline fraction of the powders by the procedure described in Section 3.2. As the result of this calculation the two parameters, σ and m corresponding to the log-normal size distribution are obtained and listed in Table II. Fig. 5 shows the grain-size distribution function, $f(x)$, corresponding to the calculated m and σ values of the crystalline fraction of the as-synthesized powder and the samples heat-treated at 1350 and 1500°C. It can be established that for the powders crystallized at temperatures up to 1450°C

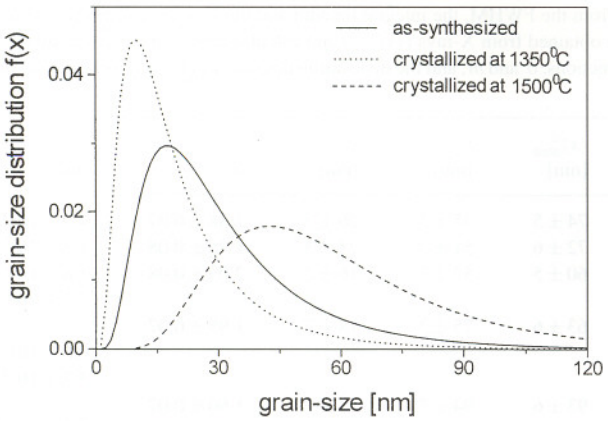

Figure 5 The grain-size distribution function, $f(x)$, of the crystalline fraction of the as-synthesized powder and the samples heat-treated at 1350 and 1500°C.

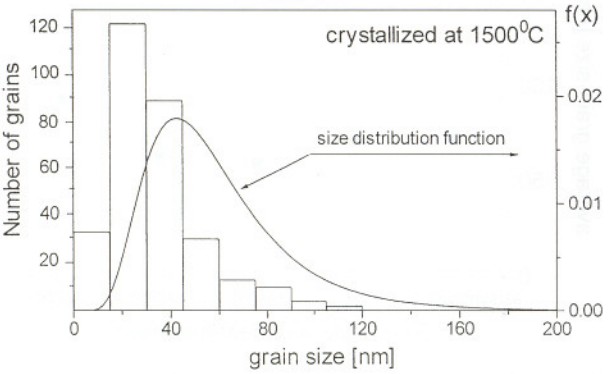

Figure 6 Bar-diagram of the size distribution obtained from TEM micrographs and the size distribution function, $f(x)$ (solid line), determined by X-rays for powder heat-treated at 1500°C.

the median (m) of the size distribution decreased and the variance (σ) increased. It was probably occuring because of the crystallization of the smaller amorphous grains. After the heat-treatment at 1500°C the median of the size distribution increased and the variance decreased because of the extensive grain-coarsening in the sample. The log-normal size-distribution function corresponding to the σ and m values for the powder heat-treated at 1500°C is shown as solid line in Fig. 6. The size distribution obtained from the TEM micrographs is shown as bar-graph in Fig. 6. (The scales of the bar-diagram and the size-distribution function are on the left- and the right hand side of the figure.) In the TEM measurements 300 particles were chosen at random in different areas in the powder. A typical TEM micrograph of this powder is shown in Fig. 7. The agreement between the bar-diagram and the size-distribution function is good. The small quantitative difference between the X-ray and the TEM results is probably due to the facts that the bar-diagram was obtained from a relatively small number of grains and that the smaller particles of the amorphous phase were not taken into account in the size distribution function determined by X-rays. To increase the number of grains for counting in TEM micrographs would need formidably greater efforts. About five orders of magnitude more grains contribute to the X-ray measurements. The good qual-

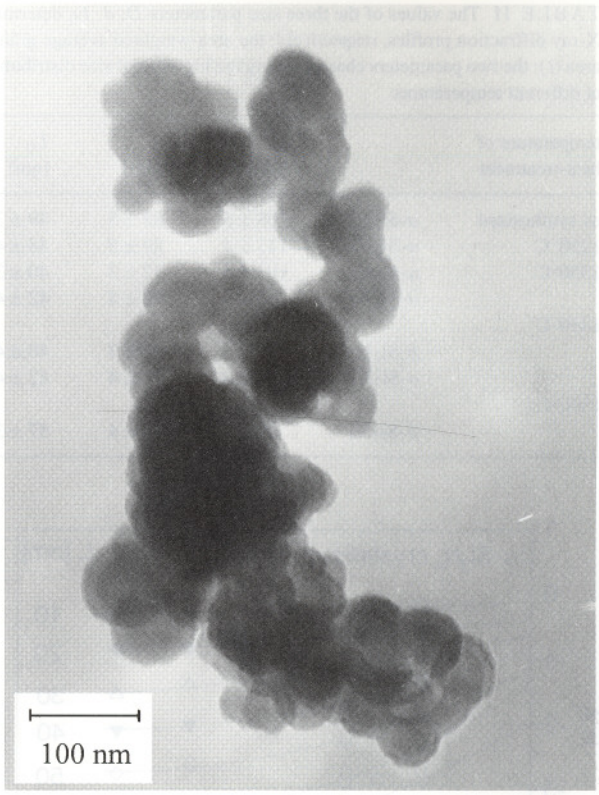

Figure 7 TEM micrograph of powder crystallized at 1500°C.

itative and quantitative agreement between the TEM and X-ray determined size distributions indicates that i) the size distribution is log-normal in accordance with observations by other authors in many nanocrystalline materials [6, 14, 28], ii) the X-ray procedure described in Section 3.2 yields the size distribution in good agreement with direct observations.

The dislocation density has been determined from the *modified* Warren-Averbach plot as follows [7, 8]. The second coefficients in the quadratic regression to the Fourier coefficients provide the values of $\rho B L^2 \ln(R_e/L)$ as a function of L (see Equation 3). Plotting $\rho B \ln(R_e/L)$ versus $\ln L$ enables the graphic determination of ρ and R_e. The dislocation densities obtained for α-Si_3N_4 and β-Si_3N_4 are listed in Table II. The dislocation densities were found to be of the order of magnitude between 10^{14} and 10^{15} m^{-2}. It can be seen that there is no significant change in the dislocation density for α-Si_3N_4 during heat-treatment and β-Si_3N_4 had a bit higher dislocation density than α-Si_3N_4.

5. Conclusions

Nanodisperse silicon nitride powder was synthesized by vapor phase reaction of silicon tetrachloride and ammonia in a thermal plasma reactor and crystallized at temperatures 1250, 1350, 1450 and 1500°C. The effect of crystallization on the phase content, the average grain-size and the grain-size distribution was studied.

1. At crystallization temperatures up to 1350°C α-Si_3N_4 crystallized from the predominantly amorphous silicon nitride powder while the amount of β-Si_3N_4 did not change. At temperatures above 1350°C

the crystalline content of the samples became very high ($\geq$75 vol%) and both α- and β-Si_3N_4 crystallized from the amorphous phase.

2. The average grain-size of the amorphous phase is lower than that of the crystalline fraction in the as-synthesized state. It was shown that the grain-size of the amorphous phase increased during heat-treatments. The average size of the crystalline grains decreased slightly at temperatures up to 1450°C probably because of the crystallization of the smaller amorphous grains, while it significantly increased during heat-treatment at 1500°C. The average grain-size of the entire powder increases with increasing temperature that is caused by the grain-coarsening in the amorphous phase and the increase of the amount of the crystalline phase having large grains. For the powder having high amount of crystalline phases (crystallized at 1500°C) the average grain-size of the crystalline fraction obtained by X-rays agrees well with that of the entire powder calculated from the specific surface area.

3. The size distribution obtained by X-rays was in good agreement with that determined by TEM for the powder having high crystalline phase content (crystallized at 1500°C). It was shown that for the materials crystallized at temperatures up to 1450°C the median (m) of the size distribution decreased and the variance (σ) increased probably because of the crystallization of the smaller amorphous grains. After the heat-treatment at 1500°C the median of the distribution increased and the variance decreased because of the extensive grain-coarsening in the sample.

4. The dislocation densities were found to be of the order of magnitude between 10^{14} and 10^{15} m^{-2}. β-Si_3N_4 had a bit higher dislocation density than α-Si_3N_4.

Acknowledgements

The authors are indebted to Dr. Katalin Tasnady for the TEM measurements. The authors are grateful for the financial support of the Hungarian Scientific Research Fund, OTKA, Grant Nos. D-29339 and T029701 and the Hungarian Government Fund FKFP 0116/1997.

References

1. J. SZÉPVÖLGYI and I. MOHAI, *Ceram. Int.* **25** (1999) 711.
2. G. ZIEGLER, J. HEINRICH and G. WÖTTING, *J. Mat. Sci.* **22** (1987) 3041.
3. G. PETZOW and R. SERSALE, *Pure and Applied Chemistry* **59** (1987) 1674.
4. J. SZÉPVÖLGYI and I. MOHAI, in "Engineering Ceramics'96: Higher Reliability through Processing," edited by G. N. Babini *et al.* (Kluwer Academic Publishers, Dordrecht, The Netherlands, 1997) p. 89.
5. F. CAMBIER, A. LERICHE, E. GILBART, R. J. BROOK and F. L. RILEY, in "The Physics and Chemistry of Carbides, Nitrides and Borides," edited by R. Freer (Kluwer Academic Publishers, Dordrecht, The Netherlands, 1990) p. 13.
6. C. E. KRILL and R. BIRRINGER, *Phil. Mag. A* **77** (1998) 621.
7. T. UNGÁR and A. BORBÉLY, *Appl. Phys. Lett.* **69** (1996) 3173.
8. T. UNGÁR, S. OTT, P. SANDERS, A. BORBÉLY and J. R. WEERTMAN, *Acta Mater.* **46** (1998) 3693.
9. T. UNGÁR, I. DRAGOMIR, Á. RÉVÉSZ and A. BORBÉLY, *J. Appl. Cryst.* **32** (1999) 992.
10. M. WILKENS, *Phys. Stat. Sol. (a)* **104** (1987) K1.
11. I. GROMA, T. UNGÁR and M. WILKENS, *J. Appl. Cryst.* **21** (1988) 47.
12. P. KLIMANEK and R. KUZEL JR., *ibid.* **21** (1988) 59.
13. R. KUZEL JR. and P. KLIMANEK, *ibid.* **21** (1988) 363.
14. T. UNGÁR, A. BORBÉLY, G. R. GOREN-MUGINSTEIN, S. BERGER and A. R. ROSEN, *Nanostructured Materials* **11** (1999) 103.
15. J. SZÉPVÖLGYI and I. MOHAI, *J. Mater. Chem.* **5** (1995) 1227.
16. J. SZÉPVÖLGYI, F. L. RILEY, I. MOHAI, I. BERTOTI and E. GILBART, *ibid.* **6** (1996) 1175.
17. C. P. GAZZARA and D. R. MESSIER, *Ceram. Bull.* **56** (1977) 777.
18. N. CAMUSCU, D. P. THOMPSON and H. MANDAL, *J. European Ceram. Soc.* **17** (1997) 599.
19. M. WILKENS and H. ECKERT, *Z. Naturforschung* **19a** (1964) 459.
20. B. C. LIPPENCA and M. A. HERMANNS, *Powd. Met.* **7** (1961) 66.
21. A. GUINIER, "X-ray Diffraction" (Freeman, San Francisco, CA, 1963).
22. T. UNGÁR and G. TICHY, *Phys. Stat. Sol. (a)* **171** (1999) 425.
23. CH.-M. WANG, X. PAN, M. RUEHLE, F. L. RILEY and M. MITOMO, *J. Mater. Sci.* **31** (1996) 5281.
24. K. RAJAN and P. SAJGALIK, *J. Am. Ceram. Soc.* **17** (1997) 1093.
25. B. E. WARREN, *Progr. Metal Phys.* **8** (1959) 147.
26. M. RAND, J. I. LANGFORD and J. S. ABELL, *Phil. Mag. B* **68** (1993) 17.
27. A. J. C. WILSON, "X-ray Optics" (Methuen, London 1962).
28. CH. D. TERWILLIGER and Y. M. CHIANG, *J. Am. Ceram Soc.* **78** (1995) 2045.

Received 21 December 1999
and accepted 23 February 2000